

Effective Homogeneous Hydrolysis of Phosphodiester and DNA Cleavage by Chitosan-copper Complex

Zhang, Qi^a(张琦) Xiang, Yan^{*a,b}(相艳) Yang, Ruxin^b(杨汝新)
Si, Jiangju^a(司江菊) Guo, Hong^b(郭红)

^a School of Materials Science and Engineering, Beihang University, Beijing 100191, China

^b School of Chemistry and Environment, Beihang University, Beijing 100191, China

We aimed to explore the role of chitosan-based metal complexes in catalyzing the hydrolysis of phosphodiester. To this end, we performed detailed studies on the kinetics of the chitosan copper complex (CSCu)-catalyzed hydrolysis of bis(4-nitrophenol) phosphate (BNPP) in Tris-H⁺ buffer and in an organic solvent. A significant enhancement in the rate of reaction (up to 3×10^5 -fold acceleration) was observed at pH 8.0 (25 °C). The pH dependence of BNPP hydrolysis at pH 5.5–9.5 and the UV spectra revealed that the copper-bounded water molecules underwent deprotonation to form the active catalytic species CSCu-OH. The kinetic behavior of BNPP catalytic hydrolysis in the Tris-H⁺ buffer was consistent with that predicted by the Michaelis-Menten kinetics model. An intramolecular nucleophilic attack by the copper-bonded hydroxide group on the same activated phosphodiester substrate was proposed as the catalytic mechanism for CSCu-catalyzed reaction system. The results of DNA binding and cleavage experiments indicated electrostatic binding mode of CSCu to DNA as well as the strong capability of CSCu to disturb the supercoiled strand of DNA and cleave it to nicked circular form.

Keywords homogeneous catalysis, chitosan, copper, kinetics, phosphodiester, hydrolysis

Introduction

The phosphodiester bonds of DNA are exceptionally resistant to hydrolysis under physiological conditions, and it is extremely difficult to find new catalysts that can accelerate the rate of hydrolysis. Mimicking the activities of nucleases is an attractive research area in molecular biology and therapy, since nucleases play an essential role in the activity of artificial restriction enzymes and the conformational probes of nucleic acids.¹

In the past decade, efforts to mimic the activities of nucleases have led to the development of numerous functional models for the hydrolysis of phosphodiester bonds.² The reaction mechanism of hydrolase and the effect of metal ions on the active center are important aspects in inorganic chemistry studies. Many recent studies have sought to understand the mechanism of the rate enhancement induced by these reagents. Most of the model systems for phosphate-ester cleavage utilize inner- or outer transition metal complexes. Indeed, compounds containing metals from the transition series, particularly Zn(II),³ Cu(II),⁴ and Co(III),⁵ and the lanthanide series⁶ have been used as model compounds. Previous studies have shown that the observed enhancement in the rate of phosphate-ester hydrolysis can be primarily attributed to the ability of the ligand-bound

metal ions to polarize water molecules; these polarized water molecules are more acidic than the free water molecules, facilitating an attack on the phosphorus center. These studies have identified the features of the model compounds that contribute to faster phosphate ester cleavage. In the model compounds, the ligand is expected to provide a site for the metal ions and facilitate the catalytic reaction. As the results of previous studies have indicated, metals usually combine with a variety of macrocyclic and acyclic polydentate ligands.⁷ The metal center is expected to possess a site for coordination with the phosphate ester and a water ligand, which undergoes deprotonation to form a coordinated hydroxide⁸ that acts as a nucleophile to attack the phosphate ester.

Chitosan, a natural polysaccharide, has been widely used in biotechnological, pharmaceutical, as well as enzyme immobilization procedures.⁹ However, the viability of using chitosan as a ligand for supporting a hydrolytic catalyst has been rarely studied. Recently, heterogeneous hydrolysis of phosphodiester by copper-chelated chitosan magnetic nanocarrier was studied by Dong-Hwang Chen.¹⁰ We previously reported catalytic kinetic studies of *N*-cetyl-*O*-sulfated-chitosan copper complex as an artificial hydrolase of phosphodiester.¹¹ However, the chitosan-based catalysts^{10,11} in

* E-mail: xiangy@buaa.edu.cn; Tel./Fax: 0086-010-82339539

Received September 25, 2011; revised November 26, 2011; accepted December 13, 2011.

Project supported by the National Natural Science Foundation of China (Nos. 20403002, 20773008), the Beijing Novel Program (No. 2008B12) and the National High-Tech R&D Program (No. 2007AA05Z146).

previous reports are water-insoluble and the catalytic activity might be limited by the heterogeneous system. In order to extend the potential of using chitosan as the backbone of an artificial enzyme, we prepared water-soluble chitosan-based copper complex (CSCu) and investigated the kinetics of a series of hydrolytic reactions of bis(4-nitrophenyl) phosphate (BNPP) that were catalyzed by CSCu. Chitosan showed sufficient coordination with the copper ions; moreover, its molecular chain may construct a suitable microenvironment for the catalytic reaction. In this paper, we have analyzed the result of kinetic studies and discussed a proposed hydrolytic mechanism for the catalytic reaction. The copper ions in the catalytic system may be responsible for the activation of the coordinated water molecule, which is followed by a nucleophilic attack of the copper-hydroxo complex on the substrate. We also identified the fine ability of CSCu to DNA binding and cleavage by UV-Vis scan and gel electrophoresis.

Experimental

Materials

Chitosan powder [water-soluble, made in China by Hai De Bei Co. Ltd.; average molecular weight determined by gel-permeation chromatography (GPC), 6300 g/mol] was used without further purification. The degree of deacetylation of the amino groups was 75%; the moisture content in the chitosan powder was 3% (w/w). Bis(4-nitrophenyl) phosphate (BNPP), tris(hydroxymethyl)aminomethane (Tris-base) and calf thymus DNA (CT DNA) were purchased from Sigma Aldrich. Plasmid pUC19 DNA (0.5 $\mu\text{g}/\mu\text{L}$) and Loading buffer for gel electrophoresis were purchased from Takara Co. Ltd. GelRed (gene green) was purchased from Biotium. Inc. Agarose was from Gene Tech Co. Ltd. Dialysis membrane (molecular weight cut off: 3500) was from Beijing Reida Henghui Tech. Co. Ltd. All reagents, unless otherwise indicated, were of analytical grade and were used without further purification. Tris- H^+ buffer was used to avoid the influence of the chemical components, and in each experimental run, the pH of the buffer was adjusted by adding analytically pure hydrochloric acid. The buffer system was not sensitive to the polarity of solvent system, and its pK_a value did not show any significant changes.

Preparation of chitosan copper complex

A specific amount of chitosan was dissolved in water. Then, copper chloride solution was added to the reaction vessel. The mixed solution was stirred continuously for 4 h at 50 $^{\circ}\text{C}$; the solution was then dialyzed for 48 h to remove any unreacted copper ions. The dialyzed was freeze-dried and vacuum dried to obtain the multinuclear chitosan copper complex.

Characterization

The GPC system model used for the molecular

weight measurement of chitosan was Shimadzu LC-20A Series Gel Permeation Chromatography system equipped with a pump (LC-20-AD) and a refractive index (RI) detector (RID-10A). The analysis was performed on a PL Gel column (Agilent) using water as the mobile phase. The flow rate was 1.0 mL/min, and the temperature was maintained at 40 $^{\circ}\text{C}$. The concentration of the sample used for the analysis was 2 mg/mL. The average molecular weight of chitosan was tested to be 6300 g/mol.

Fourier-transform infrared was used to characterize the differences between chitosan and CSCu FTIR spectra were obtained with a Perkin-Elmer FTIR 1600 series spectrometer, and all the samples were prepared as potassium bromide pellets. IR (KBr) for chitosan ν : 3415, 2920, 1630, 1520, 1018 cm^{-1} . IR (KBr) for CSCu ν : 3435, 2920, 1630, 1510, 1020, 470 cm^{-1} . XPS data were recorded using a PHI 1600 XPS Surface Analysis System (Physical Electronics, Eden Prairie, MN). The samples were placed in vacuum (10^{-8} – 10^{-7} Pa), and the analyzed area was \varnothing 6 μm – \varnothing 6 mm. We used the following scanning conditions: 6.80 ms/step, 0.6 eV/step, and 6 sweeps. The survey spectra were obtained using an average of 10 scans with a pass energy of 26.95 eV and running from 0 to 1100 eV. XPS data for CSCu see Table 1.

Table 1 Binding energy of N, O and Cu for CS and CSCu

Sample	N_{1s}	O_{1s}	$\text{Cu}_{2p_{1/2}}$	$\text{Cu}_{2p_{3/2}}$
CS	399.2	400.8	531.4	—
CS—Cu	399.7	401.6	531.6	932.7
$\text{CuCl}_2 \cdot 2\text{H}_2\text{O}$	—	—	—	934.2

The copper content in the complex was detected by inductively coupled plasma-atomic emission spectroscopy (ICP-AES) by using Intrepid II XSP with the following parameters: RF power, 1150 W; nebulizer flow, 26.0 PSI; and auxiliary air pressure, 1.0 LPM. The copper content w of the chitosan copper complex was 2.82%.

Kinetics of BNPP hydrolysis

The pH of the reaction solutions was adjusted with Tris- H^+ buffer (0.01 $\text{mol} \cdot \text{L}^{-1}$) and appropriate amounts of sodium hydroxide stock solution. The chitosan copper complexes were dissolved in the solutions, and the pH value of the reaction solutions was measured at room temperature (25 $^{\circ}\text{C}$). The samples were prepared by using the procedure described in a previous section and incubated at (25.0 \pm 0.2) $^{\circ}\text{C}$ prior to the analysis. The initial substrate concentration was 0.05–1 $\text{mmol} \cdot \text{L}^{-1}$. The ligand and metal-ion concentration varied from 0.0–2.0 $\text{mmol} \cdot \text{L}^{-1}$. The reactions were initiated by adding 20 μL of a 1.5 $\text{mmol} \cdot \text{L}^{-1}$ solution of BNPP (solid substrate dissolved in acetonitrile) into an efficiently stirred sample solution. The reactions were monitored by detecting the increase in the absorption

band for the *p*-nitrophenolate anion at 400 nm (ϵ , 16980 mol \cdot L $^{-1}\cdot$ cm $^{-1}$; pK_a , 6.98), and this increase was monitored immediately after injection of the substrate. The reported data are the average of duplicate measurements, with reproducibility >50%. The initial-slope method was used to determine the pseudo-first-order rate constants. The initial rate of the reaction was obtained by calculating the slope of a linear plot of 4-nitrophenolate concentration versus time ($R > 0.995$). Reaction rate was tested with respect to both metal complex and BNPP, and the rate constants were determined from the initial rates.

DNA binding studies

Solution of calf thymus DNA (CT DNA) gave a ratio of UV absorbance, A_{260}/A_{280} of 1.8–1.9 : 1, indicating that the DNA was sufficiently free of protein.^{4g,12} The stock solution of CT-DNA was prepared in Tris-HCl/NaCl (Tris-H $^+$) buffer, pH 8.0 (stored at 4 °C and used within 7 d). The DNA concentration per nucleotide was determined by absorption spectroscopy using the molar absorption coefficient (6600 mol \cdot L $^{-1}\cdot$ cm $^{-1}$) at 260 nm.

All CD spectroscopic studies were carried out with a continuous flow of nitrogen purging the polarimeter, and the measurements were performed at room temperature with 1 cm pathway cells. The CD spectra were run from 800 to 200 nm at 50 nm/min and the buffer background was subtracted automatically. The average of three independent scans was taken as the final CD spectrum of each sample. Data were recorded at 0.1 nm intervals. The CD spectrum of CT-DNA (100 μ mol \cdot L $^{-1}$) alone was recorded as the control experiment.

pUC19 DNA cleavage

Cleavage of supercoiled pUC19 DNA by CSCu was investigated by agarose gel electrophoresis. Tris-H $^+$ (pH=8.0, 10 mmol \cdot L $^{-1}$) buffer was used. Reactions were performed by incubating DNA at 25 °C in the presence/absence of increasing CSCu for 1 h. All reactions were quenched by loading buffer (4 μ L). Agarose gel electrophoresis was carried out on a 1.0% agarose gel in 0.5 \times TBE (Tris-boracic acid-EDTA) buffer containing 0.5 μ g/mL GelRed at a constant voltage of 100 V for 120 min. The gels were visualized in an electrophoresis documentation and analysis system 120.

Results and discussion

Phosphodiester hydrolysis promoted by the chitosan copper complex

We tabulated the representative pseudo-first-order rate constants for the hydrolysis of BNPP by CS, CSCu, and copper salts in Tris-H $^+$ buffer at 25 °C (Table 2).

The spontaneous hydrolytic rate of BNPP is extremely low, with a rate constant of 1.1×10^{-10} s $^{-1}$ at pH 8.0, and OH $^-$ is the nucleophile in the spontaneous hydrolysis.¹³ The pseudo-first-order kinetics showed

Table 2 Kinetic data for BNPP hydrolysis by different catalysts

Catalyst	Spontaneous hydrolysis ¹³	Buffer	Cu $^{2+}$	CS	CSCu
$k_{\text{obs}}/\text{s}^{-1}$	1.1×10^{-10}	4.8×10^{-7}	9.1×10^{-7}	4.2×10^{-7}	5.0×10^{-6}

^a [BNPP], 1×10^{-4} mol \cdot L $^{-1}$; [Cu $^{2+}$], 0.1 mmol \cdot L $^{-1}$; 10 mmol \cdot L $^{-1}$ Tris-H $^+$; pH, 8.0; temperature, 25 °C.

that there was a continuous increase in the absorption at 400 nm versus the reaction time, which suggested that the catalytic function of the CSCu complex was enhanced when an excess of the phosphodiester substrate was present in the reaction system. The CSCu-catalyzed hydrolysis of BNPP showed a significant rate enhancement (4.5×10^4 -fold) in comparison with the rate of spontaneous hydrolysis. Moreover, in the Tris-H $^+$ buffer solution, the CSCu-catalyzed reaction showed a 10-fold rate enhancement, which was relative to the rate of the uncatalyzed reactions.

The order of the reaction with respect to the catalyst was determined. CSCu-catalyzed phosphodiester hydrolysis showed a pseudo-first-order dependence, which has been explored in detail (Figure 1). The rate of hydrolysis of BNPP showed linear dependence on catalyst concentration at low concentrations (Figure 1, inset), and we obtained a pseudo-first-order rate constant (k_{obs}) of 3.6×10^{-5} s $^{-1}$, which was calculated using the rate law ($v_0 = k_{\text{obs}}[\text{S}]$). At catalyst concentrations greater than 2×10^{-4} mol \cdot L $^{-1}$, the reaction showed a decreased reaction order (less than 1). This observation can be explained by the competition between the substrate and water to coordinate with the catalyst. Similar kinetic behavior was observed when the substrate was in excess in the reaction system.

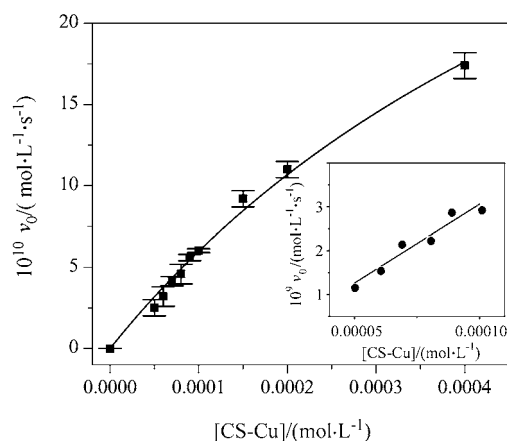
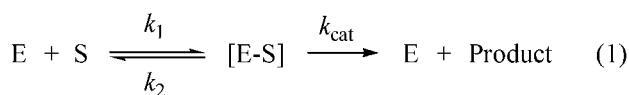


Figure 1 Effect of CSCu concentration on the initial rate of BNPP hydrolysis. The initial concentration of BNPP was 5×10^{-4} mol \cdot L $^{-1}$ in 10 mmol \cdot L $^{-1}$ Tris-H $^+$ (pH 8.0, 25 °C). The inset is a graph of the data points at low catalyst concentrations; the data points were fit to the line by using the linear least-squares method (correlation coefficient, 0.995).

In normal enzyme catalytic reactions, the reaction starts with the binding of the substrate with the enzyme

to form an intermediate with a binding constant k_1 , a process that has been described with Eq. (1). This is followed by hydrolysis, and the products are released, with k_{cat} as the decomposition rate constant of the rate-limiting step [Eq. (2)]. The rate law for the reaction can be obtained by using Eq. (3), with an assumption that the concentration of the bound substrate (S) in the solution is much less than that of the free substrate.



$$v_0 = \frac{k_{\text{cat}}[\text{CSCu}][\text{S}]}{[\text{S}] + K_M} \quad (2)$$

$$v_0 = \frac{k_1 k_{\text{cat}}[\text{CSCu}][\text{S}]}{k_1[\text{S}] + k_{-1} + k_{\text{cat}}} \quad (3)$$

In order to gain a better insight into the mechanism of the CSCu-catalyzed reaction, the initial rate was measured as a function of the substrate concentrations. The hydrolysis of BNPP by CSCu, which is a first-order reaction at lower concentrations of BNPP, was slightly saturated at higher concentrations (Figure 2). The saturation-kinetics plot represents the substrate coordination to the CSCu complex, which occurred according to Eq. (2). Considering that the binding of the catalyst to the substrate must have occurred rather quickly ($k_1 \gg k_{-1} \gg k_{\text{cat}}$), the initial rate can be expressed by Eqs. (3) and (4). The experimental data were consistent with the results obtained by using Eq. (4), the Lineweaver-Burk function [Eq. (5) and Figure 2 inset], and the results from the equation $K_M = (k_{-1} + k_{\text{cat}})/k_1$. We also determined the following values from this analysis: Michaelis constant (K_M), $(2.3 \pm 0.1) \text{ mmol} \cdot \text{L}^{-1}$; maximal velocity (v_{max}), $(3.6 \pm 0.2) \times 10^{-8} \text{ mol/L} \cdot \text{s}$; binding constant (k_1), $1355 \text{ mol} \cdot \text{L}^{-1}$; reverse-reaction constant (k_{-1}), 3.0 s^{-1} ; and first-order rate constant for the decomposition of the intermediate Cu(II)-hydroxide-phosphate complex (k_{cat}), $5.2 \times 10^{-5} \text{ s}^{-1}$.

$$\frac{1}{v} = \frac{K_M}{v_{\text{max}}} + \frac{1}{v_{\text{max}}[\text{S}]} \quad (4)$$

$$k_{\text{obs}} = \frac{K_{\text{H}_2\text{O}}[\text{H}^+] + K_{\text{OH}}K_a}{[\text{H}^+] + K_a} \quad (5)$$

Effects of pH on the hydrolysis of BNPP

The pH value is an important factor for the active species in catalytic hydrolysis system. In order to identify the reactive species, we obtained UV-Vis spectra of CSCu in aqueous systems with different pH values. As shown in Figure 3, the absorption peak at 233 nm was enhanced with an increase in the pH values. This phenomenon indicated the formation of hydroxyl species in

the alkaline solution.

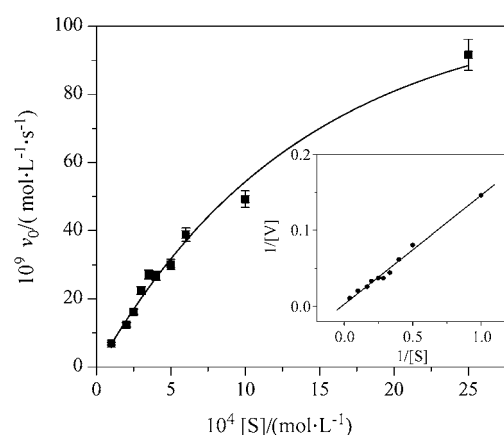


Figure 2 Dependence of v_0 on the concentration of BNPP. The initial concentration of CSCu was $1 \times 10^{-4} \text{ mol} \cdot \text{L}^{-1}$ in $10 \text{ mmol} \cdot \text{L}^{-1}$ Tris- H^+ ; pH, 8.0; temperature, $25 \text{ }^\circ\text{C}$. When the BNPP concentration was greater than $5.0 \times 10^{-4} \text{ mol} \cdot \text{L}^{-1}$, the CSCu-catalyzed hydrolysis of BNPP occurred in the saturation-kinetics mode. The data were consistent with those obtained by the Michaelis-Menten equation; the inset is the Lineweaver-Burk plot, with a linear correlation coefficient of 0.995.

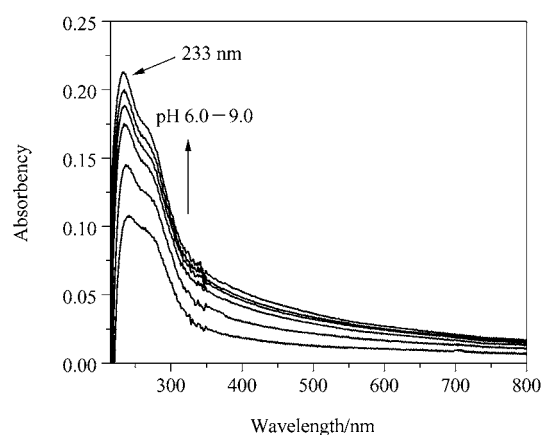


Figure 3 UV-Vis spectra of the reaction system at different pH values. UV-Vis (CSCu-OH) λ_{max} : 233 nm. The amount of CSCu-OH was enhanced with an increase pH values.

We studied the catalytic cleavage of BNPP at pH values between 5.5 and 9.5 and found that the initial rates of cleavage increased with an increase in pH values, especially when $\text{pH} > 6.5$. The graph of pH versus v_0 showed a typical sigmoidal curve (Figure 4). The kinetic behavior was consistent with the previous observation that the water molecules coordinating with copper ions underwent deprotonation in an alkaline environment, leading to the generation of Cu-OH as the catalytic species or nucleophile.^{10-11,14} On the basis of these results, we hypothesized the ionization kinetics represented in Scheme 1, in which CSCu-H₂O and CSCu-OH are the active species involved in the reaction, and $K_{\text{H}_2\text{O}}$ and K_{OH} represent the rate constants for BNPP catalytic hydrolysis of the respective species.

K_a was the disassociation constant for the chelated water molecule. The relationship between pseudo rate constant and the concentration of H^+ in the reaction system has been expressed in Eq. (5). The experimental data were consistent with the results obtained using Eq. (5) and the representation of data in the inset of Figure 4, and the obtained K_{H_2O} and K_{OH} values were $1.5 \times 10^{-6} s^{-1}$ and $1.6 \times 10^{-5} s^{-1}$, respectively. We also derived a pK_a value of (8.0 ± 0.2) , corresponding to the CSCu-bound water molecule, from Eq. (5). It was apparent that the coordinated water molecule was less active than the deprotonated product. Therefore, in our studies, the CSCu-bound hydroxyl group was expected to be the most effective nucleophile in a weak alkaline solution. When $pH < 6.5$, the deprotonation was inhibited; consequently, the CSCu- H_2O would be the primary catalytic species, with a lower hydrolytic rate.

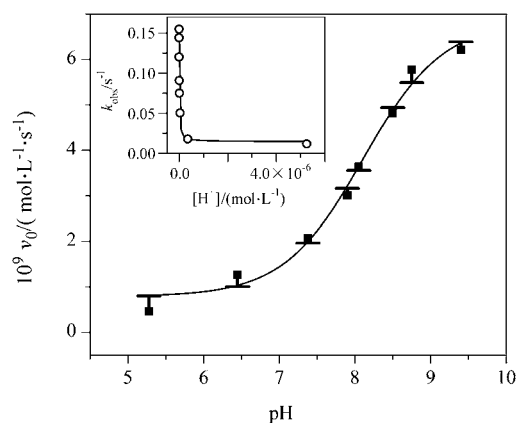
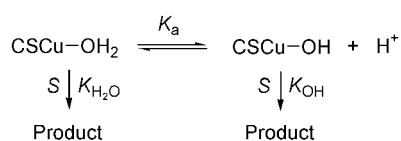


Figure 4 Graph of the influence of pH on the catalytic hydrolysis of BNPP. $[CSCu]$, $1 \times 10^{-4} mol \cdot L^{-1}$; $[BNPP]$, $1 \times 10^{-4} mol \cdot L^{-1}$; $10 mmol \cdot L^{-1}$ Tris- H^+ ; temperature, $25 ^\circ C$. The data are fitted to a theoretical curve that is shown in the inset, with pK_a , 8.0 ± 0.2 ; k_{OH} , $1.6 \times 10^{-5} s^{-1}$; and K_{H_2O} , $1.5 \times 10^{-6} s^{-1}$.

Scheme 1 Proposed deprotonation of the CSCu-bound water molecule



In order to achieve the better understanding of the role of water molecules in the catalytic process, we performed the catalytic hydrolysis in an acetonitrile system with a fixed concentration of water. The initial rate for BNPP hydrolysis (v_0) was obtained, as shown in Figure 5. On the basis of the previously obtained results, we used a substrate concentration of $1 \times 10^{-4} mol \cdot L^{-1}$ and a catalyst concentration of $2.5 \times 10^{-5} - 2 \times 10^{-4} mol \cdot L^{-1}$; the reaction behavior in the aqueous solution showed that v_0 was related to the concentration of CSCu. Using Eq. (3), the binding constant (k_1) and decomposition rate constant (k_{cat}) for the reaction in the acetonitrile system were calculated to be $1.6 \times 10^4 mol \cdot L^{-1}$ and

$7.3 \times 10^{-5} s^{-1}$, respectively. The k_1 value was more than 10 times higher than the corresponding value for the aqueous solution (k_1), showing that the association between Cu and the substrate in the acetonitrile system was much faster than that in the aqueous solvent. However, there was no significant difference between the k_{cat} value and the corresponding value (k_{cat}) of the aqueous system. These results suggested that the water molecule might compete with the substrate during the coordination with the copper ion. However, water molecules did not show any significant effect on both k_{cat} value and the cleavage of the leaving groups, which suggested that the intramolecular attack was mainly caused by the copper-bound hydroxyl groups.¹⁵

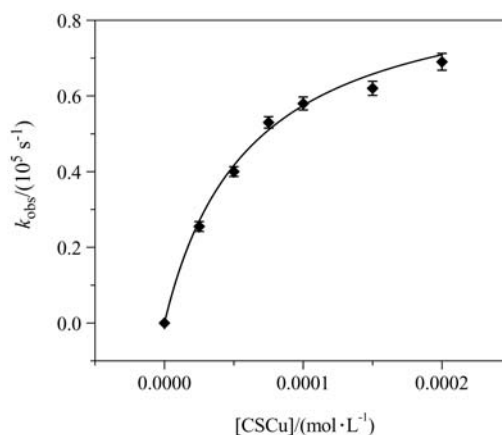


Figure 5 Effect of catalyst concentration on BNPP hydrolysis in organic solvent in the presence of $0.5 mol \cdot L^{-1} H_2O$. Initial concentration of the substrate was $1 \times 10^{-4} mol \cdot L^{-1}$. $pH 8.0$, $25 ^\circ C$.

Mechanism of BNPP hydrolysis

On the basis of the results of XPS and FT-IR, we proposed structure of the CSCu complex was one in which the copper ion coordinates with the two glucosamine groups on the chitosan-backbone chains; two hydroxyl groups occupy two other empty orbits, forming a tetra-coordinated structure, as shown in Figure 6. The result was consistent with the DFT study conducted by Terreux.¹⁶

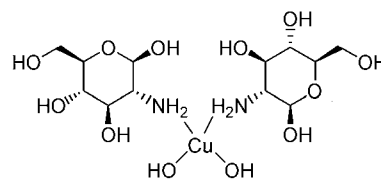
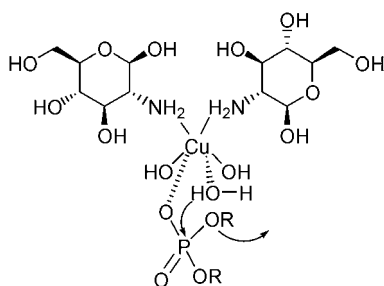


Figure 6 Proposed coordinated structure of CSCu.

In the CSCu-promoted hydrolysis reaction, the high affinity between the PO bond of the substrate and the metal active-center is demonstrated by the binding constant ($k_1 = 1355 mol \cdot L^{-1}$). The association of the CSCu-bonded hydroxyl with the substrate, after which

the copper ions activate the substrate and the bound water molecule, further polarizing the P—O bonds for the next nucleophilic attack, forms the intermediate. Equilibrium exists between the deprotonation and protonation of Cu-H₂O; at higher pH values, deprotonation is the primary pathway, leading to the generation of more efficient nucleophile Cu—OH, which attacks the active P—O bond, cleaving the nitrophenyl anion. The reaction ended and restarted simultaneously. The proposed intramolecular nucleophilic mechanism has been represented in Scheme 2. The interaction between the copper ions and the phosphorus atom can be enhanced by the hydroxyl groups on the chitosan pyranose ring and the two chelated hydroxyl groups, which would be helpful in the following nucleophilic attack. The experimental data for the organic solvent also provided the evidence for the intramolecular nucleophilic attack.

Scheme 2 Proposed mechanisms for the BNPP hydrolysis by CSCu. Due to the high affinity, the substrate rapidly coordinated with the active copper center, which was followed by the internal hydroxide attack on the P atom.



Interaction between CSCu and DNA molecular

UV-Vis spectra are used to investigate interaction between the DNA molecular and CSCu. As shown in Figure 7, CT-DNA in Tris-H⁺ buffer has absorption bands at 260 nm. Upon addition of an increasing amount of CSCu (from 5 to 25 μmol·L⁻¹) to DNA solution (20 μg/mL), an obvious increasing absorption at 260 nm was observed. This change indicates there was stereo configuration variation of the DNA molecular which was caused by the binding of DNA with CSCu. As a natural cationic polymer, there are abundant active groups, e.g., hydroxyl, amino groups in the molecular chain, chitosan itself has fine ability to bind with negative charged phosphate groups in the backbone of DNA molecular. And its high affinity of CSCu to DNA could be enhanced by the deprotonation of copperbound water molecular in alkaline solution. Thus, we demonstrated that the association of CSCu to DNA mainly was caused by the strong electrostatic interaction. Additionally, part of hydrogen bonds between the base pairs of DNA might be breached by this strong interaction. The distinct hyperchromicity of the UV spectra suggests that supercoiled molecular chain of DNA became relaxed after it interacted with CSCu and more and more base pairs were exposed that induced the increasing absorption. Thus we proposed that CSCu might bind with

DNA molecular by the strong electrostatic interaction and the dimensional configuration of DNA might be altered.

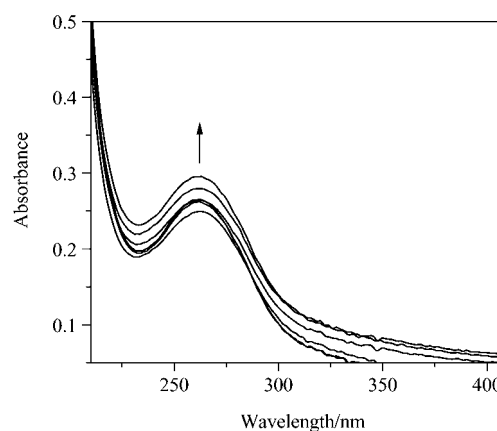


Figure 7 Absorption spectra of CT-DNA in the presence of increasing amounts of CSCu. ([DNA]=20 μmol·L⁻¹, [CSCu]=0–25 μmol·L⁻¹, 10 mmol·L⁻¹ Tris-H⁺ buffer, pH 8.0, 25 °C). The Arrows shows the absorbance enhanced with increasing CSCu concentration.

The further studies of circular dichroism (CD) also proved that CSCu has effect on the structure of CT DNA. As shown in Figure 8, the CD spectra of CT-DNA were changed after it was treated by CSCu ([CSCu]/[DNA]=1 : 1) for 5 min, the negative band (245 nm) and the positive band (276 nm) decreased with addition of CSCu which means CSCu is effective in perturbing the secondary structure of DNA. This suggests CSCu can unwind the DNA helix and lead to the loss of helicity. Additionally, the result of CD also indicated the fine ability of CSCu to combine with DNA molecular which was described by Eq. (2) we mentioned in kinetics studies.

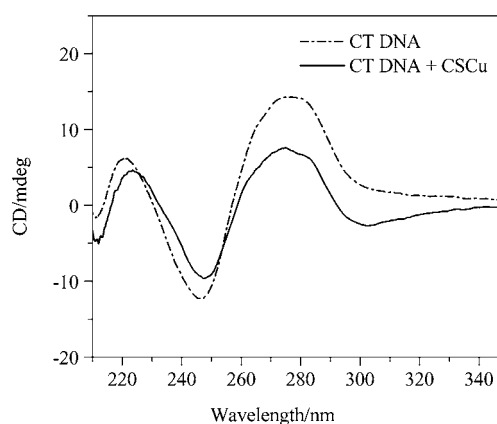


Figure 8 CD spectra of CT DNA (1.0 × 10⁻⁴ mol·L⁻¹) and the interaction with CSCu ([CSCu]/[DNA]=1). The spectra were recorded in 10 mmol·L⁻¹ Tris-H⁺ buffer; solid line was recorded by incubating the CT-DNA with CSCu for 5 min, pH 8.0 and 25 °C.

DNA cleavage

Considering CSCu as artificial phosphodiesterase, the cleavage experiment on natural DNA has been carried by agarose gel electrophoresis, supercoiled pUC19 DNA used as the substrate. We adopted CSCu with different concentration to cleave pUC19 DNA molecular. The reactions were carried out by incubating the complex with pUC 19 DNA for 1 h in Tris-H⁺ (pH=8.0). The result in Figure 9 indicated that the supercoiled DNA molecular can be cleaved into nicked and linear DNA by CSCu complex, which was evidenced by the disappearance of form I (supercoiled form) of the plasmid and the appearance of the form II (nicked circular form). The observed rate constant k_{obs} for pUC19 DNA cleavage by CSCu, obtained from Figure 9, is 0.079 h^{-1} , a rate acceleration of 6 orders of magnitude over uncatalyzed DNA hydrolysis.⁵ On the basis of the catalytic kinetics studies and DNA binding and cleavage experiments, we proposed that the negative charged phosphate group in DNA strands is the most active binding site to bind with CSCu. The existence of copper ions facilitates the binding of CSCu to DNA, generates an attacking nucleophilic reactant and promotes cleavage of DNA strands. Thus, it can be regarded that the intermediate CSCu-DNA complex was formed very quickly, followed by the intramolecular nucleophilic attack on the phosphodiester bond of DNA backbone which induced the DNA cleavage.

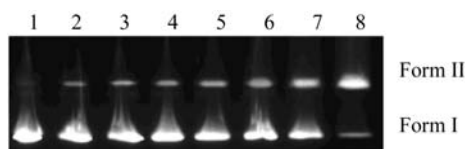


Figure 9 Agarose gel electrophoresis of cleavage reaction of pUC19 DNA ($20 \mu\text{mol}\cdot\text{L}^{-1}$ bp) by CSCu. Scission condition: lane 1: DNA control, the concentration of CSCu: lane 2, $5 \mu\text{mol}\cdot\text{L}^{-1}$; lane 3, $10 \mu\text{mol}\cdot\text{L}^{-1}$; lane 4, $20 \mu\text{mol}\cdot\text{L}^{-1}$; lane 5, $30 \mu\text{mol}\cdot\text{L}^{-1}$; lane 6, $40 \mu\text{mol}\cdot\text{L}^{-1}$; lane 7, $50 \mu\text{mol}\cdot\text{L}^{-1}$; lane 8, $100 \mu\text{mol}\cdot\text{L}^{-1}$; incubation time, 1 h; $10 \text{ mmol}\cdot\text{L}^{-1}$ Tris-H⁺ buffer, pH 8.0 at 25°C .

Conclusion

As a natural polymer, chitosan has a unique molecular structure and chemical properties that can be exploited in catalyst design. In this paper, we tentatively used the chitosan-based copper complex as an artificial hydrolase to catalyze phosphodiester BNPP hydrolysis and natural DNA cleavage. The results of our investigation highlighted the capability of CSCu as artificial catalytic model. BNPP hydrolysis by CSCu in aqua solution showed significant rate enhancement (3×10^5 -fold) over its spontaneous hydrolysis. The kinetics of CSCu-catalyzed BNPP hydrolysis was consistent with those predicted by the Michaelis-Menten model. Moreover, CSCu has been found to alter configuration structure of DNA strand and promote DNA cleavage

efficiency under mildness conditions. On the basis of kinetics studies and spectrum analysis as well as gel electrophoresis, electrostatic of DNA binding is suggested for CSCu, the active species of copper-bound hydroxide group and the intramolecular attack mechanism are proposed for CSCu-catalyzed reaction system. We concluded that chitosan-based metal complexes have potential application as a catalyst for cleavage of phosphodiester bonds, since they show relative high catalytic efficiency, and are relatively cheaper and environment-friendly.

References

- (a) Shelton, V. M.; Morrow, J. R. *Inorg. Chem.* **1991**, *30*, 4295.
(b) Rammo, J.; Schneider, H.-J. *Inorg. Chim. Acta* **1996**, *251*, 125.
(c) Molenveld, P.; Engbersen, J. F. J.; Reinhoudt, D. N. *Angew. Chem., Int. Ed.* **1999**, *38*, 3189.
(d) Chen, X. Q.; Peng, X. J.; Wang, J. Y. *Eur. J. Inorg. Chem.* **2007**, *34*, 5400.
- (a) Erkkila, K. E.; Odom, D. T.; Barton, J. K. *Chem. Rev.* **1999**, *99*, 2777.
(b) Branum, M. E.; Tipton, A. K.; Zhu, S.; Que, L. *J. Am. Chem. Soc.* **2001**, *123*.
(c) Komiyama, M.; Kina, S.; Matsumura, K. *J. Am. Chem. Soc.* **2002**, *124*, 13731.
(d) Scheffer, U.; Strick, A.; Ludwig, V.; Peter, S.; Kalden, E.; Göbel, M. W. *J. Am. Chem. Soc.* **2005**, *127*.
- (a) Bruice, T. C.; Tsubouchi, A.; Dempcy, R. O.; Olson, L. P. *J. Am. Chem. Soc.*, **1996**, *118*, 9867.
(b) Iranzo, O.; Kovalevsky, A. Y.; Morrow, J. R.; Richard, J. P. *J. Am. Chem. Soc.*, **2003**, *125*.
(c) Li, C. L.; Hor, L. I.; Chang, Z. F.; Tsai, L. C.; Yang, W. Z.; Yuan, H. S. *Embo J.* **2003**, *22*.
(d) Feng, G.; Mareque-Rivas, J. C.; Torres Martin, R.; Williams, N. H. *J. Am. Chem. Soc.*, **2005**, *127*, 13470.
- (a) Hegg, E. L.; Deal, K. A.; Kiessling, L. L.; Burstyn, J. N. *Inorg. Chem.* **1997**, *36*, 1715.
(b) Young, M. J.; Wahnou, D.; Hynes, R. C.; Chin, J. *J. Am. Chem. Soc.* **1995**, *117*, 9441.
(c) Chin, K. O. A.; Morrow, J. R. *Inorg. Chem.* **1994**, *33*, 5036.
(d) Detmer, C. A.; Pamatong, F. V.; Bocarsly, J. R. *Inorg. Chem.* **1997**, *36*, 3676.
(e) Cacciapaglia, R.; Casnati, A.; Mandolini, L. *J. Am. Chem. Soc.* **2007**, *129*, 12512.
(f) Selmeczi, K.; Giorgi, M.; Speier, G.; Farkas, E.; Reglier, M. *Eur. J. Inorg. Chem.*, **2006**, 1022.
(g) Shao, Y.; Sheng, X.; Li, Y.; Jia, Z. L.; Zhang, L. L.; Lin, F.; Lu, G. Y. *Bioconjugate Chem.* **2008**, *19*, 1840.
- Hettich, R.; Schneider, H.-J. *J. Am. Chem. Soc.* **1997**, *119*, 5638.
- (a) Aguilar-Perez, F.; Gomez-Tagle, P.; Collado-Fregoso, E.; Yatsinirsky, A. K. *Inorg. Chem.* **2006**, *45*, 9502.
(b) Kou, X. M.; Hu, Y.; Huang, Z.; Meng, X. G.; Zeng, X. C. *Chin. J. Chem.* **2005**, *23*, 1303.

- (c) Zhang, Y. Q.; Liu, F.; Xiang, Q. X. *Int. J. Chem. Kinet.* **2004**, *36*, 687.
- 7 (a) Shionoya, M.; Kimura, E.; Shirot, M. *J. Am. Chem. Soc.* **1993**, *115*, 6730.
(b) Burstyn, J. N.; Deal, K. A. *Inorg. Chem.* **1993**, *32*, 3585.
(c) Xiang, Q.-X.; Yu, X.-Q.; Su, X.-Y.; Yan, Q. S.; Wang, T.; You, J. S.; Xie, R. G. *J. Mol. Catal. A: Chem.* **2002**, *187*, 195.
(d) Kong, D. Y.; Martell, A. E.; Reibenspies, J. *Inorg. Chim. Acta* **2002**, *333*, 7.
(e) Fry, F. H.; Fischmann, A. J.; Belousoff, M. J.; Spiccia, L.; Brugger, J. *Inorg. Chem.* **2005**, *44*, 941.
(f) Huang, Y.; Chen, S. Y.; Zhang, J.; Tan, X. Y.; Jiang, N.; Zhang, J. J.; Zhang, Y.; Lin, H. H.; Yu, X. Q. *Chem. Biodivers.* **2009**, *6*.
- 8 Kimura, E.; Hashimoto, H.; Koike, T. *J. Am. Chem. Soc.* **1996**, *118*, 10963.
- 9 (a) Lim, S.-H.; Hudson, S. M. *Carbohydr. Res.* **2004**, *339*, 313.
(b) Foresti, M. L.; Ferreira, M. L. *Enzyme Microb. Technol.* **2007**, *40*, 769.
- 10 Chang, Y.-C.; Chen, D.-H. *React. Funct. Polym.* **2009**, *69*.
- 11 Xiang, Y.; Zhang, Q.; Si, J. J.; Du, J. P.; Guo, H.; Zhang, T. *J. Mol. Catal. A: Chem.* **2010**, *322*.
- 12 Zhao, Y. M.; Zhu, J. H.; He, W. J.; Yang, Z.; Zhu, Y. G.; Li, Y.; Zhang, J. F.; Guo, Z. *Chem. Eur. J.* **2006**, *12*.
- 13 Hanafy, A. I.; Lykourinou-Tibbs, V., *Inorg. Chim. Acta*, **2005**, *358*, 1247.
- 14 Morrow, J. R.; Trogler, W. C. *Inorg. Chem.* **1988**, *27*, 3387.
- 15 Kaminskaia, N. V.; He, C.; Lippard, S. J. *Inorg. Chem.* **2000**, *39*, 3365.
- 16 Terreux, R.; Domard, M.; Viton, C.; Domard, A. *Biomacromolecules* **2006**, *7*, 31.

(E100 Zhao, X.; Fan, Y.)